

## ORIGINAL ARTICLE

## Vasohibin 2 is transcriptionally activated and promotes angiogenesis in hepatocellular carcinoma

X Xue<sup>1,5</sup>, W Gao<sup>1,5</sup>, B Sun<sup>1</sup>, Y Xu<sup>1</sup>, B Han<sup>2</sup>, F Wang<sup>1</sup>, Y Zhang<sup>1</sup>, J Sun<sup>1</sup>, J Wei<sup>1</sup>, Z Lu<sup>1</sup>, Y Zhu<sup>1</sup>, Y Sato<sup>3</sup>, Y Sekido<sup>4</sup>, Y Miao<sup>1</sup> and Y Kondo<sup>4</sup>

Hepatocellular carcinoma (HCC) typically relies on angiogenesis for its malignant behavior, including growth and metastasis. Vasohibin 2 (VASH2) was previously identified as an angiogenic factor, but its role in tumorigenesis is unknown. Using quantitative PCR and western blot analyses, we found that *VASH2* is overexpressed in HCC cells and tissues. Using chromatin immunoprecipitation, we detected histone modifications at the putative *VASH2* promoter, with increased H3K4 trimethylation and H3 acetylation and decreased H3K27 trimethylation, suggesting that epigenetic mechanisms are responsible for the deregulated *VASH2* transcription in HCC. Knockdown of *VASH2* via siRNA inhibited the proliferation of the hepatoma cell lines by delaying cell cycle progression and increasing apoptosis. Importantly, we found VASH2 secreted in the culture supernatant, and co-expression of its secretory chaperone small vasohibin-binding protein (SVBP) further enhanced VASH2 secretion. The supernatant from HepG2 cells expressing VASH2 enhanced the proliferation, migration and tube formation of human umbilical vein endothelial cells, and knockdown of *VASH2* significantly inhibited these effects. In an *in vivo* study using a nude mouse model, we found that exogenous VASH2 significantly contributed to tumor growth, microvessel density and hemoglobin concentration in the tumors. Further analyses showed that the VASH2-mediated increase in the transcription of fibroblast growth factor-2, vascular endothelial growth factor and vasohibin 1 may be the mechanism underlying these effects. Taken together, these data indicate that VASH2 is abnormally expressed in HCC cells as a result of histone modifications and that VASH2 contributes to the angiogenesis in HCC via an SVBP-mediated paracrine mechanism. These results indicate a novel and important role for VASH2 in HCC angiogenesis and malignant transformation.

*Oncogene* (2013) 32, 1724–1734; doi:10.1038/onc.2012.177; published online 21 May 2012

**Keywords:** angiogenesis; vasohibin 2; hepatocellular carcinoma; histone modification

## INTRODUCTION

Hepatocellular carcinoma (HCC) is the fifth most common tumor type worldwide and the third most common cause of cancer-related deaths. However, systemic chemotherapy is not effective for the treatment of HCC. HCC typically relies on angiogenesis for its malignant behavior, including tumor growth and metastasis, and because HCC is vascularized, chemoembolization improves the survival of patients with advanced HCC. Therefore, targeting angiogenesis seems to be a promising approach for the treatment of HCC.<sup>1</sup> Vascular endothelial growth factor (VEGF)<sup>2–4</sup> is an important angiogenic factor in the hypoxic conditions associated with tumors, and anti-angiogenic agents that inhibit the VEGF pathway have been approved for the treatment of HCC (for example, Sorafenib for advanced HCC<sup>5</sup>). Unfortunately, less than half of all patients with advanced HCC benefit from these therapies, and these benefits are often only transient.<sup>6</sup> Therefore, the identification of targets other than VEGF is important for clarifying the mechanisms underlying angiogenesis in HCC and testing future therapeutic strategies.<sup>7</sup>

Vasohibin 2 (VASH2) belongs to the VASH family, which includes vasohibin 1 (VASH1) and VASH2. VASH1 is selectively induced in

endothelial cells (ECs) by angiogenic factors, such as VEGF, and operates as an intrinsic and highly specific feedback inhibitor of activated ECs engaged in angiogenesis.<sup>8</sup> Recently, VASH1 was found to be involved in angiogenesis in various solid tumors, and exogenous VASH1 significantly blocks sprouting angiogenesis by tumors.<sup>9,10</sup> VASH2 was first described by Shibuya *et al.*<sup>11</sup> In contrast with VASH1, VASH2 has been found to promote angiogenesis.<sup>12</sup>

Unlike VEGF and other angiogenic factors, VASH2 has been identified as an extrinsic and VEGF-independent angiogenic factor that is highly expressed in bone marrow-derived mononuclear cells but weakly expressed in ECs. Although its role in tumor angiogenesis is unknown, it is likely that VASH2 functions via mechanisms that are distinct from those of VEGF, which may make it a novel target for tumor therapy.

In this study, we show that *VASH2* transcription is upregulated in HCC cells via an epigenetic mechanism, and this increased expression contributes to HCC angiogenesis through paracrine effects. This study identifies a new and important role for VASH2 in HCC angiogenesis and malignant transformation and suggests that VASH2 may be a novel target for the treatment of HCC and other malignancies.

<sup>1</sup>Department of General Surgery, the First Affiliated Hospital with Nanjing Medical University, Nanjing, China; <sup>2</sup>Department of Endocrinology, Nanjing Children's Hospital Affiliated to Nanjing Medical University, Nanjing, China; <sup>3</sup>Department of Vascular Biology, Institute of Development, Aging and Cancer, Tohoku University, 4-1 Seiryomachi, Aoba-ku, Sendai, Japan and <sup>4</sup>Division of Molecular Oncology, Aichi Cancer Center Research Institute, 1-1 Kanokoden, Chikusa-Ku, Nagoya, Japan. Correspondence: Y Miao or W Gao, Department of General Surgery, the First Affiliated Hospital with Nanjing Medical University, 300# Guangzhou Road, Nanjing 210029, China or Y Kondo, Division of Molecular Oncology, Aichi Cancer Center Research Institute, 1-1 Kanokoden, Chikusa-ku, Nagoya 464-8681, Japan.

E-mail: miaoyi@njmu.edu.cn or gao11@hotmail.com or ykondo@aichi-cc.jp

<sup>5</sup>These authors contributed equally to this work.

Received 17 November 2011; revised 28 March 2012; accepted 9 April 2012; published online 21 May 2012

## RESULTS

### Increased VASH2 expression in HCC cells and tissue

We used a Taqman quantitative reverse transcription (qRT)-PCR-based strategy to measure *VASH2* expression in three HCC cell lines, the normal liver cell line L02 and human umbilical vein ECs (HUVECs). As observed in Figure 1a, qPCR showed HepG2 cells expressed *VASH2* at higher levels than normal L02 cells or HUVECs ( $P < 0.05$ ). HUVECs had a low level of *VASH2* expression, similar to the results reported by Shibuya *et al.*<sup>11</sup> Besides, western blot coincided with qPCR results except L02 showed no band and HUVECs showed very low *VASH2* expression. To confirm the expression level of *VASH2* in tissues, we also measured *VASH2* expression in 5 normal liver tissue samples and in 65 HCC tissue samples with paired adjacent non-cancerous tissue using qRT-PCR. *VASH2* expression in the normal liver tissue samples was very low but was slightly higher in the tissue adjacent to HCC tumors and significantly higher in the HCC tumors themselves. Of the 65 paired samples, 44 showed significantly higher *VASH2* expression in the cancer tissue compared with the adjacent tissue (Figure 1b,  $P < 0.05$ ). The same trend can be observed using a scatter plot (Figure 1c), which shows that the mean expression

level of *VASH2* in tumors, tumor-adjacent normal tissue and normal liver was 47.89, 12.47 and 1.54, respectively. Besides, we detected *VASH2* in clinical samples with immunohistochemistry. The result (Figure 1d) showed *VASH2* had a high expression in the tumor cells of HCC sample and almost no expression in the normal liver tissue. From the Figure 1d, we could see that *VASH2* was located in the plasma of tumor cells. Taken together, our results show that *VASH2* is highly expressed in HCC cells and tissue, indicating that *VASH2* might be activated during tumorigenesis and have an important role in HCC.

Histone modifications at the putative core promoter contribute to the activation of *VASH2* transcription

Histone modifications at promoters can form a histone code that tightly regulates gene expression.<sup>13,14</sup> H3K4 trimethylation (H3K4triMe) and H3 acetylation (H3Ac) are associated with active transcription, whereas H3K27 trimethylation (H3K27triMe) is correlated with transcriptional repression.<sup>15–17</sup> As histone modifications have been shown to be an important epigenetic mechanism underlying the deregulation of cancer-related gene expression in tumors, we investigated whether the increased

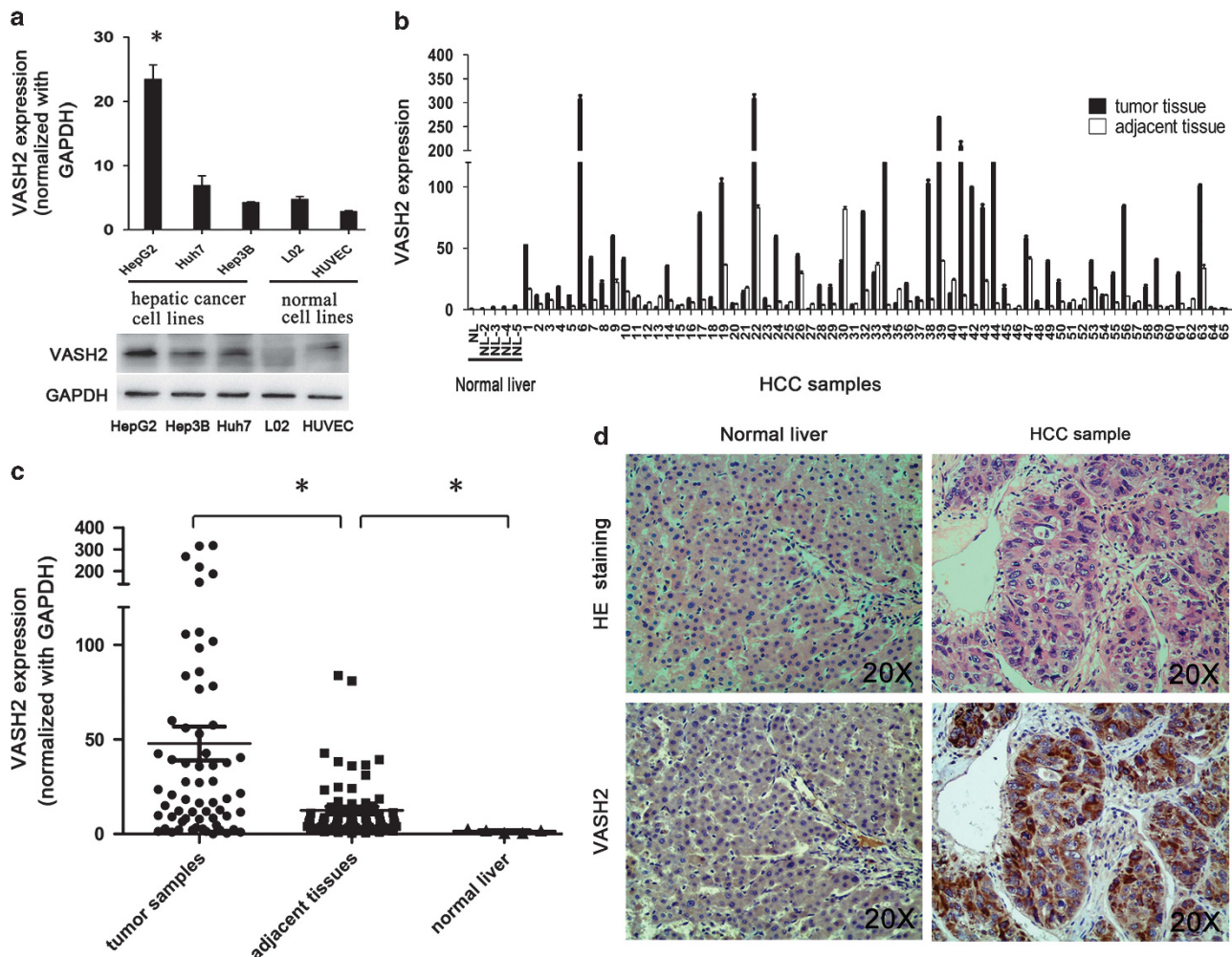


**Figure 1.** *VASH2* expression in cell lines and tissues. (a) qRT-PCR and western blot analysis of *VASH2* expression in HCC cell lines, the normal liver cell line L02 and HUVECs. HepG2 cells showed higher expression of *VASH2* than other cell lines ( $P < 0.05$ ). (b) *VASH2* expression in 5 normal liver tissues and 65 pairs of hepatic cancer tissue and adjacent tissue. Normal liver tissues had very low expression of *VASH2*, whereas the non-cancerous tissue adjacent to tumors had slightly higher expression, and hepatic cancer tissues showed the highest level of expression. Of the 65 pairs of tissues, *VASH2* expression was greater in the cancer tissue than in the adjacent tissues in 44 cases ( $P < 0.05$ ). (c) A scatter plot showing the results of *VASH2* expression in the same cancer tissue, adjacent tissue and normal liver samples (mean expression: 47.89, 12.47 and 1.54, respectively). (d) Immunohistochemistry showed *VASH2* location in the clinical HCC sample. Magnification,  $\times 20$  (\*represents  $P < 0.05$  when compared to the control group).

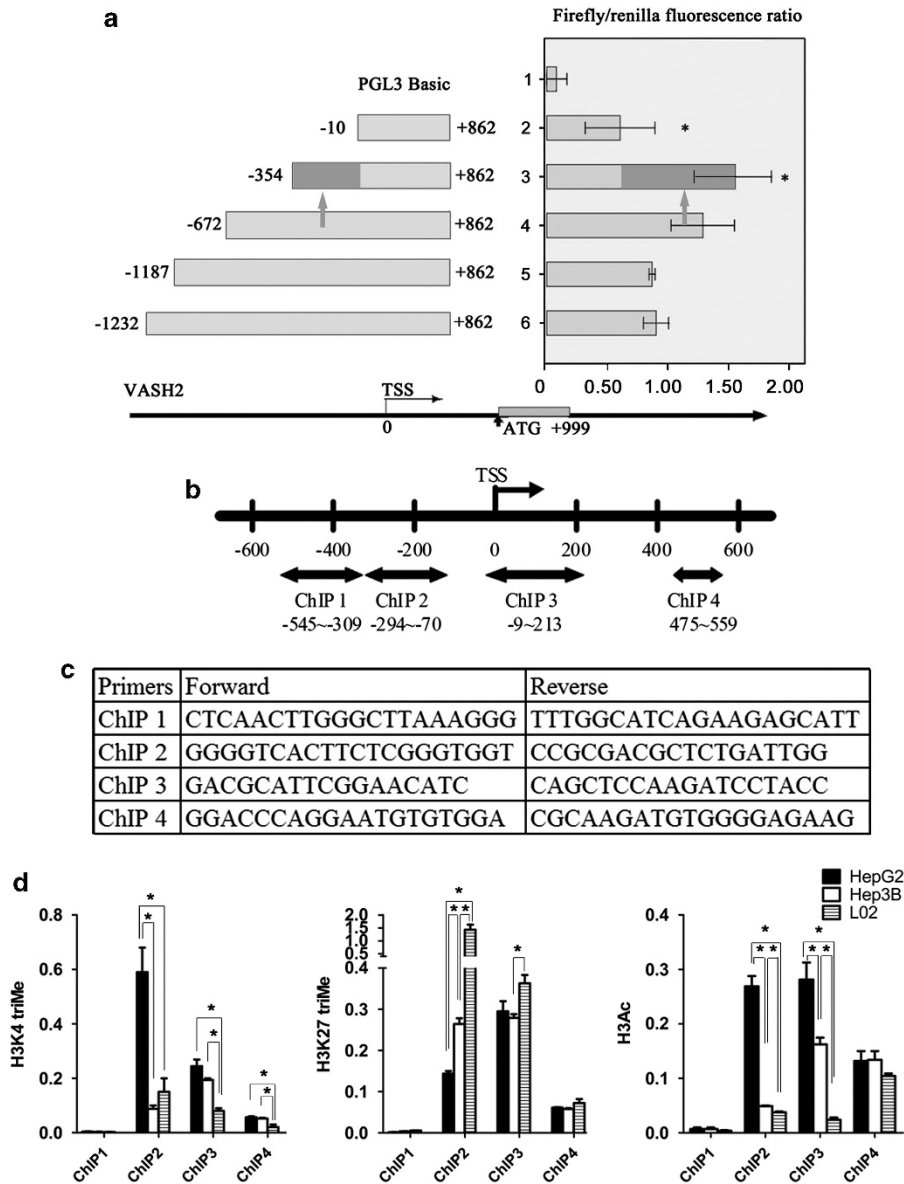


**Figure 2.** Histone modification in putative promoter of *VASH2*. **(a)** Dual luciferase reporter assay. Different segments flanking the TSS of the *VASH2* gene were amplified and ligated into the pGL3 basic vector. The plasmids were co-transfected with a *Renilla* luciferase expression plasmid into HepG2 cells, and luciferase activity was measured. The region from  $-354$  to  $+862$  had the strongest promoter activity, and the region from  $-352$  to  $-10$  seemed to be the key part (the red arrow indicates the position;  $*P < 0.05$  when compared with the control group transfected with the pGL3 basic vector). The TSS was defined to be position 0. **(b)** Map of the four real-time-PCR amplicons (ChIP 1–ChIP 4) used to analyze *VASH2* promoters by ChIP. ChIP-2 (amplifies  $-294$  to  $-70$ ) overlaps with the core promoter region ( $-352$  to  $-10$ ). **(c)** The primer sequences used to analyze the four regions of *VASH2* using ChIP. **(d)** HepG2 cells have increased levels of H3K4triMe and H3Ac and decreased levels of H3K27triMe at the *VASH2* promoter compared with Hep3B and L02 cells, while L02 showed silent histone code. The data are presented as the average of three independent experiments with the s.e. ( $*P < 0.05$  between the indicated groups). No enrichment of these four amplicons was observed in control immunoglobulin G immunoprecipitations (data not shown). A full color version of this figure is available at the *Oncogene* journal online.

expression of *VASH2* in our HCC cell lines was associated with aberrant histone modifications.

To test this, we first analyzed the putative promoter region of *VASH2* ( $-1232$  to  $+862$ , flanking the transcriptional start site (TSS)) using a luciferase reporter assay. As observed in Figure 2a, the region from  $-354$  to  $+862$  had the strongest promoter activity, and the region from  $-354$  to  $-10$  seemed to be the core part accounting for increasing promoter activity ( $P < 0.05$ ).

Next, we performed chromatin immunoprecipitation (ChIP) to compare the histone modifications around the *VASH2* promoter region in two HCC cell lines and the normal liver cells L02, HepG2 (high *VASH2* expression) and Hep3B or L02 (low *VASH2* expression).

The amplicon sizes with four primer sets are shown in Figures 2b and c. Histone-associated DNA fragments immunoprecipitated with antibodies against H3K4triMe, H3K27triMe and H3Ac were analyzed using PCR with primers designed to amplify different regions of the *VASH2* promoter. Interestingly, the region amplified using the ChIP-2 primer set, which spans the core promoter identified in the reporter assay, had a more active histone code in HepG2 cells, which have high *VASH2* expression, than the histone code in Hep3B and L02 cells, which have low *VASH2* expression. Specifically, increased H3K4triMe and H3Ac modifications and decreased H3K27triMe modifications were found; no such code was found in other examined regions (Figure 2d).



To further confirm the ChIP result, we used the 3-deazaneplanocin A (DZNep) and trichostatin A (TSA) to treat the above three cells. TSA could increase H3Ac. Although DZNep is not a specific inhibitor of EZH2, it preferentially decreases the level of H3K27me3 through the disruption of PRC2 activity. qPCR and western blot (Supplementary Figure 2S) showed that DZNep- or TSA-single-treated HepG2 had no significant change in VASH2 expression, whereas DZNep- or TSA-single-treated Hep3B and L02 had an obvious increase in VASH2 level. The combination of DZNep and TSA treatment increased the VASH2 expression in all three cells. As Hep3B and L02 had higher H3K27triMe, therefore DZNep treatment decreased the status of H3K27triMe, which recovered the VASH2 expression. This also explained why DZNep-treated HepG2 did not show the same trend because lower H3K27triMe.

These results clearly indicate that histone modifications associated with transcriptional activation were observed at the putative core promoter in HCC cell lines with high VASH2 expression, suggesting that aberrant epigenetic modifications are responsible for the increased VASH2 expression in HCC cells.

#### Generation and identification of stably transfected cells

To further address the functions of VASH2 in HCC, we over-expressed and silenced VASH2 expression. HepG2 cells with higher level of VASH2 and Hep3B with lower level of VASH2 were chosen for these experiments. We constructed VASH2 overexpression and VASH2-knockout lentiviral constructs, infected HepG2 cells and selected stably infected cells. We confirmed the expression levels using qRT-PCR and western blot (Figure 3). Stable cells of Hep3B were treated the same as HepG2 (Data were not shown).

#### VASH2 promotes proliferation of HepG2 cells *in vitro*

The growth of the stable cell lines over 5 days was determined using 3-(4,5-dimethylthiazol-2-yl)-2,5-diphenyl tetrazolium bromide assay. As shown in Figure 4a, VASH2 knockdown significantly impaired the proliferation of cells after day 3 ( $P < 0.05$ ). To further study the mechanism by which VASH2 knockdown affected proliferation, cell cycle progression and apoptosis were analyzed using flow cytometry. G2 + S% phase reflects cell proliferation ability. VASH2-knockout cells showed a delayed G2 and S phase compared with the wild-type HepG2 cells ( $49.9\% \pm 2.1\%$  vs  $40.7\% \pm 1.0\%$ ) (Figure 4b,  $P < 0.05$ ). In addition, VASH2 silencing increased the frequency of apoptosis of HepG2-shVASH2 cells ( $17.1\% \pm 1.2\%$ ) when compared with wild-type HepG2 cells ( $12.3\% \pm 1.0\%$ ; Figure 4c,  $P < 0.05$ ). Therefore, VASH2 knockdown inhibited the proliferation of HepG2 cells via a delay in cell cycle progression and increased apoptosis. We got the same result in Hep3B (Supplementary Figure 4S). These results suggest a role for VASH2 in the positive regulation of HCC cell proliferation.

#### Small vasohibin-binding protein (SVBP) facilitates VASH2 secretion by functioning as a chaperone in HCC

As VASH2 was identified as an angiogenic factor,<sup>12</sup> we hypothesized that VASH2 overexpression in HCC cells could contribute to angiogenesis in HCC, possibly via secretion from HCC cells and action on ECs in a paracrine manner. Although a previous study showed that VASH2 and VASH1 lack the classic signal sequence required for secretion, a small protein known as SVBP has been shown to aid in the secretion of VASH2.<sup>18</sup> As such, we constructed an SVBP-expressing lentivirus and infected HepG2-VASH2 and Hep3B-VASH2 cells (to generate HepG2-VASH2-SVBP and Hep3B-VASH2-SVBP, respectively). qPCR and western blot (SVBP was fused with V5 tag) showed that SVBP was overexpressed > 50-fold (Figure 5a), and overexpression of either SVBP or VASH2 did not alter the endogenous transcription of the other gene (data not shown). Supernatants were collected from

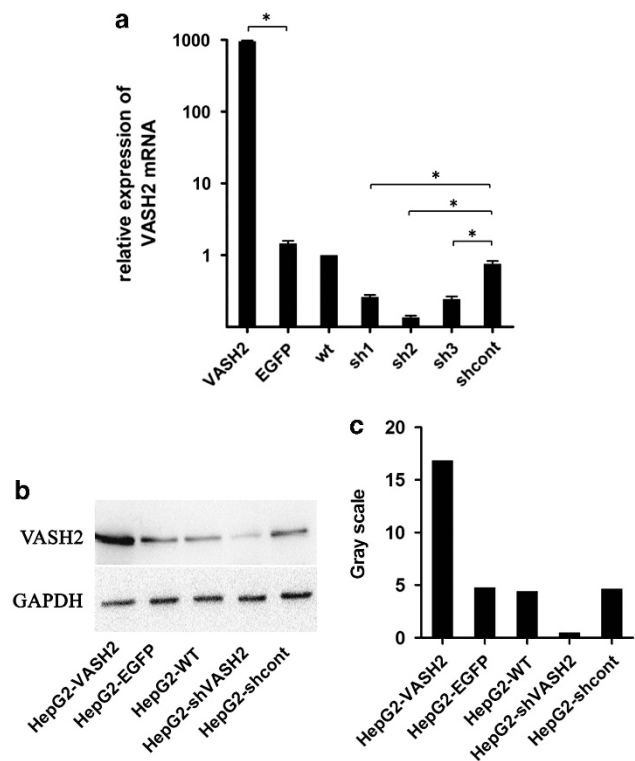


**Figure 3.** Generation and identification of stably transfected HepG2 cells. **(a)** Measurement of VASH2 expression using qRT-PCR. VASH2 indicates VASH2-overexpressing HepG2 cells; EGFP indicates HepG2 cells transfected with a vector-expressing EGFP. Wt indicates wild-type HepG2 cells. The cells transduced with the three shRNAs and one control shRNA are designated as 'sh1', 'sh2', 'sh3' and 'shcont'. VASH2-overexpressing HepG2 cells showed almost 1000-fold higher VASH2 expression than wild-type HepG2 cells, whereas VASH2-knockdown HepG2 cells had 80% lower expression when compared with wild-type HepG2 cells ( $*P < 0.05$  compared with the corresponding control group). **(b)** Western blots were used to confirm the efficiency of knockdown. The results are similar to those seen in the qRT-PCR analyses. **(c)** Gray scale analysis of the western blot data.

HepG2-VASH2-SVBP and HepG2-VASH2 cells after 24, 48 and 72 h of culture, and an enzyme-linked immunosorbent assay with VASH2 monoclonal antibody was used to quantify VASH2 secretion into the supernatant. VASH2 secretion from HepG2-VASH2-SVBP cells was significantly higher than that from HepG2-VASH2 cells, and the level in the supernatant increased with time (Figure 5b), similar to previously reported results.<sup>18</sup> Beside, we got the same results in Hep3B cells (data not shown). Following co-expression of SVBP, VASH2 secretion increased significantly, indicating that SVBP facilitates VASH2 secretion by functioning as a chaperone.

#### VASH2 promotes migration and angiogenesis of HUVECs *in vitro* in a paracrine manner

Following the confirmation of VASH2 secretion by HCC cells, its direct effect on ECs was analyzed. First, we collected supernatants from cultures of HepG2-VASH2-SVBP, HepG2-VASH2, HepG2-wt, HepG2-shVASH2 and HepG2-shcont cells after 48 h of culture, and the conditioned medium (CM) was added to adherent HUVECs. Seventy-two hours after the addition of the CM, 3-(4,5-dimethylthiazol-2-yl)-2,5-diphenyl tetrazolium assays were performed to measure HUVEC proliferation. The HepG2-VASH2-SVBP CM caused the most proliferation than HepG2-VASH2 and HepG2-wt CM, whereas the HepG2-shVASH2 CM caused less proliferation

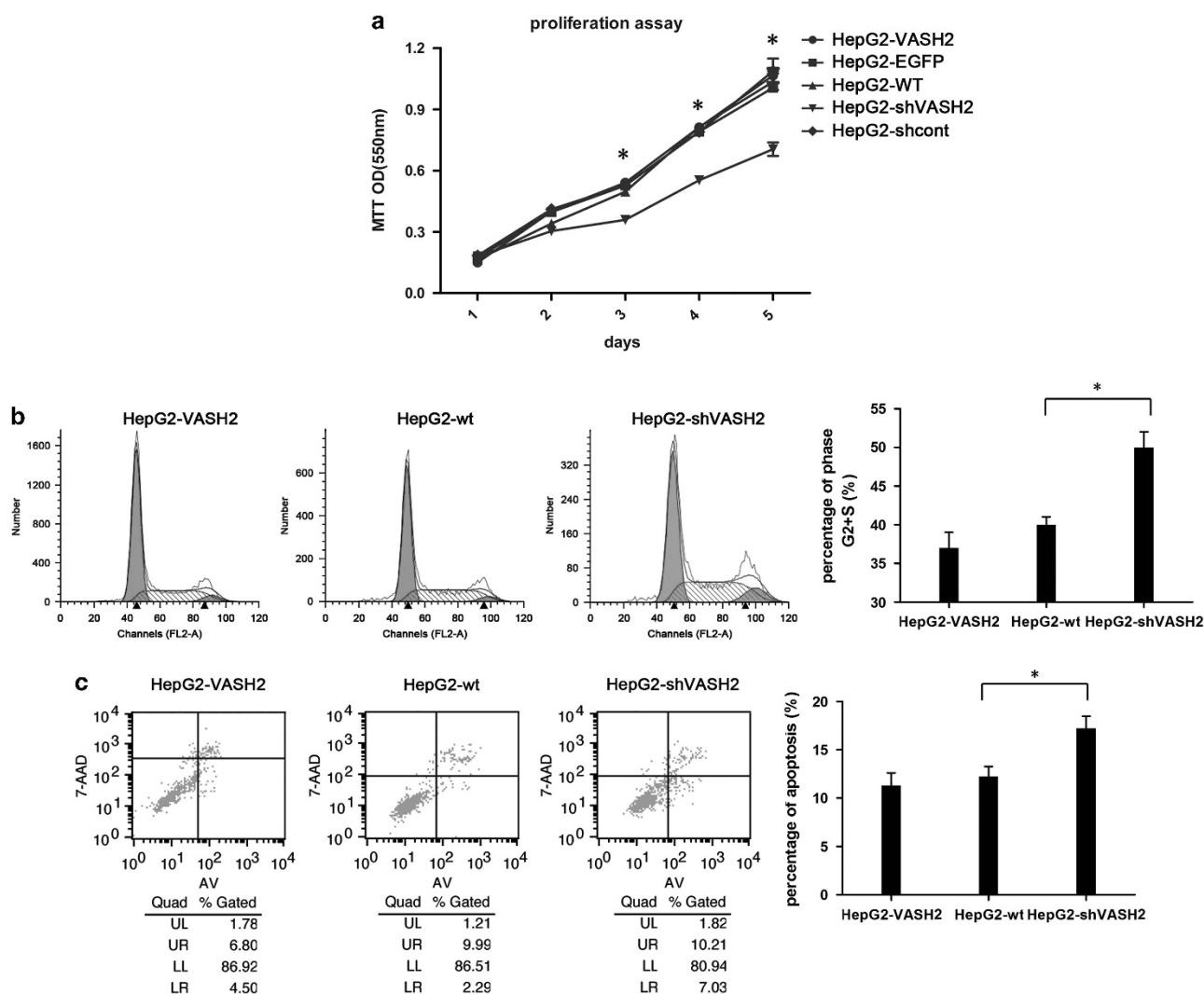


**Figure 4.** Effects of VASH2 on the proliferation of HepG2 cells. **(a)** The growth of cells over 5 days was measured using 3-(4,5-dimethylthiazol-2-yl)-2,5-diphenyl tetrazolium bromide (MTT) assays. The proliferation rate of HepG2-shVASH2 cells was significantly decreased compared with HepG2-wt cells.  $*P < 0.05$ . **(b)** Cell cycle progression was measured using flow cytometry. The progression of HepG2-shVASH2 cells was delayed in the G2 and S phase compared with HepG2-wt and HepG2-VASH2 cells. The percentage of cells in the G2 and S phase was HepG2-VASH2,  $37.2 \pm 2.0\%$ ; HepG2-wt,  $40.7\% \pm 1.0\%$ ; and HepG2-shVASH2,  $49.9\% \pm 2.1\%$ . **(c)** Apoptosis was measured using flow cytometry. The HepG2-shVASH2 cells had a higher apoptosis rate than the HepG2-VASH2 or HepG2-wt cells. ( $*P < 0.05$  compared with HepG2-wt cells). A full color version of this figure is available at the *Oncogene* journal online.

than the HepG2-shcont CM (Figure 6a,  $P < 0.05$ ). This result indicates that VASH2 promotes the proliferation of HUVECs and that the different levels of VASH2 secreted into the supernatant caused different rates of proliferation.

Next, we confirmed the effect of the CM on the migration of HUVECs using transwell chambers. The HepG2-VASH2-SVBP CM had a significantly greater ability to promote the migration of HUVECs than the HepG2-VASH2 and HepG2-wt CM, whereas the HepG2-shVASH2 CM showed less migration of HUVECs than the control group (Figures 6b and d,  $P < 0.05$ ), and the HepG2-VASH2 CM did not enhance migration compared with HepG2-wt CM.

In addition, we performed tube formation assays with the CM. We found that the HepG2-shVASH2 CM failed to promote complete network formation, whereas the HepG2-VASH2-SVBP CM promoted the most network formation than HepG2-VASH2 and HepG2-wt CM. These results suggest a role for VASH2 in the positive regulation of tube formation *in vitro* (Figures 6c and e). We obtained the similar results of Hep3B cells (Supplementary Figure 6S).

Taken together, these results demonstrate that VASH2-SVBP CM significantly increases the proliferation, migration and tube

formation of HUVECs, whereas VASH2-knockdown HCC cells CM decreases these abilities of HUVECs, indicating that VASH2 has a direct effect on HUVEC cells via a paracrine mechanism.

#### VASH2 promotes tumor growth and angiogenesis *in vivo*

To further study the effects of VASH2 on HCC proliferation and angiogenesis, *in vivo* experiments were performed via the subcutaneous transplantation of transduced cells into BALB/cA-nu nude mice. After injection, we measured the size of the growing tumors every 4 days for 20 days, after which the mice were euthanized. The tumor sizes of the HepG2-shVASH2 group were significantly smaller than the HepG2-VASH2 and HepG2-wt groups (Figure 7a). Growth curves of the tumors were also generated, and we found that after 16 days, the tumors of the VASH2-knockdown group were significantly smaller (Figure 7b). This *in vivo* result is consistent with the *in vitro* studies. The tumors were excised, and RNA was extracted to confirm that the stable transduction of VASH2 was maintained (Figure 7c). Immunohistochemical analysis using frozen sections of the tumors and a CD31-specific antibody

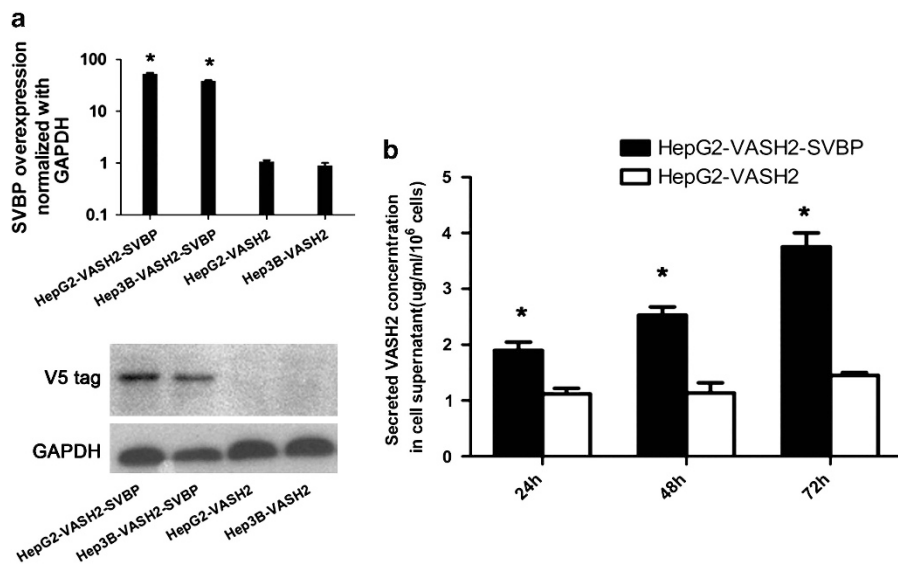


**Figure 5.** SVBP facilitates VASH2 secretion in HCC cells by functioning as a chaperone. **(a)** SVBP was transfected in HepG2-VASH2 and Hep3B-VASH2 cells. qRT-PCR and western blot was used to measure the transfection efficiency. V5 tag was fused with SVBP so that V5 antibody used as a substitute of SVBP antibody. **(b)** Overexpression of SVBP increases VASH2 secretion into the medium. VASH2 secretion was measured at three different time points using enzyme-linked immunosorbent assay. VASH2 secretion from HepG2-VASH2-SVBP cells was significantly higher than secretion from HepG2-VASH2 cells. Each group was tested in triplicate. \* $P < 0.05$  when compared with the control group.

was performed to measure the microvessel density. Each slide was evaluated with three fields, and data were analyzed as mean vessel number of these three fields. The tumors from the HepG2-shVASH2 group contained significantly fewer microvessels (Figure 7d). Hep3B had the similar results to HepG2 (Supplementary Figure 7S).

In addition, we also confirmed the angiogenic effects of VASH2 on HCC *in vivo* using Matrigel plug assays. HepG2-VASH2, HepG2-wt and HepG2-shVASH2 cells were suspended in a Matrigel/Dulbecco's modified Eagle's medium (DMEM) mixture and subcutaneously injected into mice. Consistent with the previous results, the HepG2-shVASH2 cells formed significantly fewer vessels compared with the HepG2-VASH2 and HepG2-wt cells (Figure 8a). Furthermore, the hemoglobin concentration was measured following Matrigel dissolution. The HepG2-shVASH2 group also showed significantly lower levels of hemoglobin (Figure 8b,  $P < 0.05$ ). We had the similar results of Hep3B cells (Supplementary Figure 8S).

These data indicate that knockdown of VASH2 significantly inhibits tumor growth and angiogenesis, indicating that VASH2 has a role in promoting HCC proliferation and angiogenesis. Interestingly, the HepG2-VASH2 group did not show greater tumor growth or angiogenesis than the HepG2-wt group. This might reflect the fact that wild-type HepG2 cells already have relatively high VASH2 expression or that enhancing angiogenesis via a paracrine mechanism is pivotal for VASH2 to affect tumor growth. Exogenous overexpression of VASH2 did not alter its secretion because VASH2 expression does not alter SVBP expression.

VASH2 promotes angiogenesis through fibroblast growth factor (FGF)-2 and VEGF via autocrine and paracrine mechanisms. FGF-2 and VEGF are the most common angiogenic factors; therefore, we further explored whether VASH2 promoted angiogenesis through FGF-2 or VEGF. HepG2 cells expressing different levels of VASH2 and HUVECs were cocultured, and qRT-PCR was used to measure FGF-2, VEGF and VASH1 expression in the HepG2 cells and HUVECs. The HepG2-VASH2-SVBP cells, which secreted the most VASH2 increased FGF-2 (Figures 9a and b), VEGF (Figures 9c and d) and VASH1 (Figures 9e and f) expression both in the

HepG2 cells and HUVECs (\* $P < 0.05$  compared with HepG2-VASH2). In contrast, the HepG2-shVASH2 cells decreased FGF-2 (Figures 9a and b), VEGF (Figures 9c and d) and VASH1 (Figures 9e and f) expression at some of the time points ( $P < 0.05$  compared with HepG2-wt). This result indicates that secreted VASH2 might exert its effects on both HepG2 cells and HUVECs through autocrine and paracrine mechanisms. High levels of secreted VASH2 in HepG2-VASH2-SVBP cultures caused increases in FGF-2 and VEGF expression, which partly explains why VASH2 promoted angiogenesis *in vitro* and *in vivo*. At the same time, this suggests that SVBP is very important for VASH2 secretion. Interestingly, we also found that VASH1 expression was significantly increased, especially in HepG2-VASH2-SVBP cells, whereas other HepG2 cells had very low expression levels of VASH1. In addition, secreted VASH2 increased VASH1 expression in HUVECs. This phenomenon might give us a hint that there exists a dynamic balance of mutual restraint between angiogenic and anti-angiogenic factors. Increasing VASH2 may feedback to enhance VASH1 expression, similar to VEGF-mediated VASH1 upregulation.

## DISCUSSION

Our studies demonstrate that VASH2 is highly expressed in HCC cell lines and tissues and promotes HCC angiogenesis and malignant transformation. We also explored the mechanism underlying the transcriptional activation of VASH2. We analyzed the histone modifications present at the putative promoter of VASH2. Promoter activity was mainly localized to the -354 to -10 region, upstream of the TSS, and activating histone modifications (that is, increased H3K4triMe and H3Ac and decreased H3K27triMe) were found in this region, indicating that an epigenetic mechanism may be responsible for the increased VASH2 expression in HCC. This epigenetic regulation pattern is very similar to that of the *Pax7* gene in satellite cells during muscle regeneration.<sup>19</sup> We hypothesized there may be a functional element located within the region -354 to -10, while histone modification facilitates this region for binding of trans factors, which deserves further investigation.



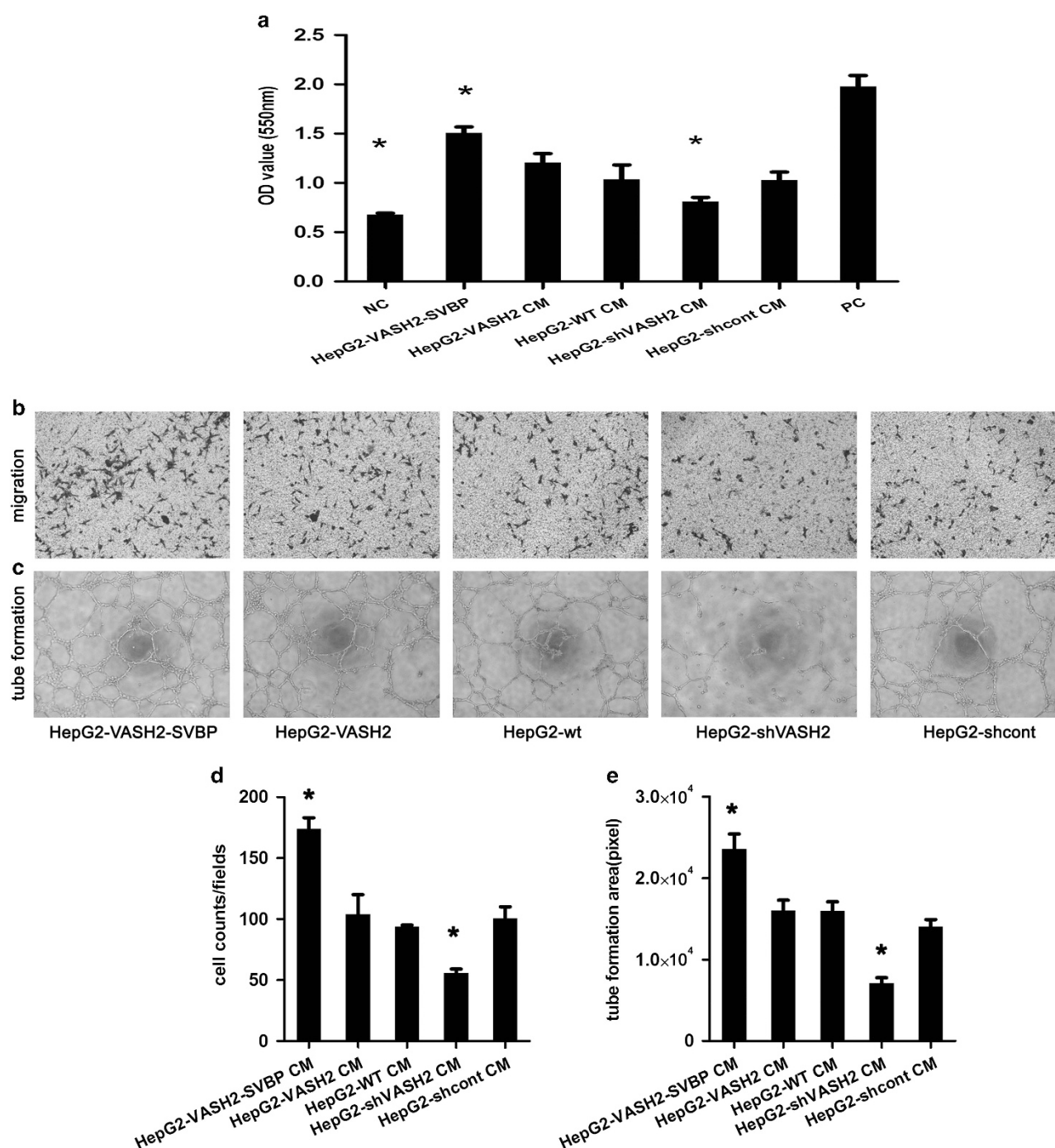


**Figure 6.** The effect of conditioned medium from different HepG2 cell lines on HUVECs. (a) Supernatant was collected from different HepG2 cell lines and added to HUVECs. 3-(4,5-Dimethylthiazol-2-yl)-2,5-diphenyl tetrazolium bromide assay showed the HepG2-VASH2-SVBP CM promoted the proliferation of HUVECs more than the HepG2-VASH2 and HepG2-wt CM, whereas HepG2-shVASH2 decreased the proliferation of HUVECs compared with the control ( $P < 0.05$ ). The positive control (PC) was 10% fetal bovine serum-DMEM, and the negative control (NC) was DMEM. (b, d) A migration assay was performed. The lower chambers were seeded with various HepG2 cell lines, and the upper chambers were seeded with  $10^4$  HUVECs. The membranes of the chambers were stained with 0.1% Crystal violet, and four fields of each membrane were photographed and counted. (c, e) Tube formation assays. HUVECs ( $2 \times 10^5$  cells) were suspended in 100  $\mu$ l CM and added to a Matrigel-coated surface. After 18 h, photos were taken and analyzed. \* $P < 0.05$ . Each group was analyzed in triplicate, and the data are presented as the average  $\pm$  s.d. A full color version of this figure is available at the *Oncogene* journal online.

VASH1, which is produced and secreted by vascular ECs, regulates EC proliferation and migration in an autocrine manner that is facilitated by SVBP. We found that supernatants from HepG2 cells have direct effects on HUVECs; therefore, we hypothesized that VASH2 requires from secretion to exert its effects. As VASH2 lacks a classic secretion signal sequence, we

hypothesized that SVBP could function as a secretion chaperone for VASH2.

Similar to the results of Suzuki *et al.*,<sup>18</sup> we found constitutive expression of SVBP in HCC cells under basal conditions, and co-expression of SVBP increased VASH2 secretion. Therefore, the mechanism underlying VASH2 secretion might be the same as

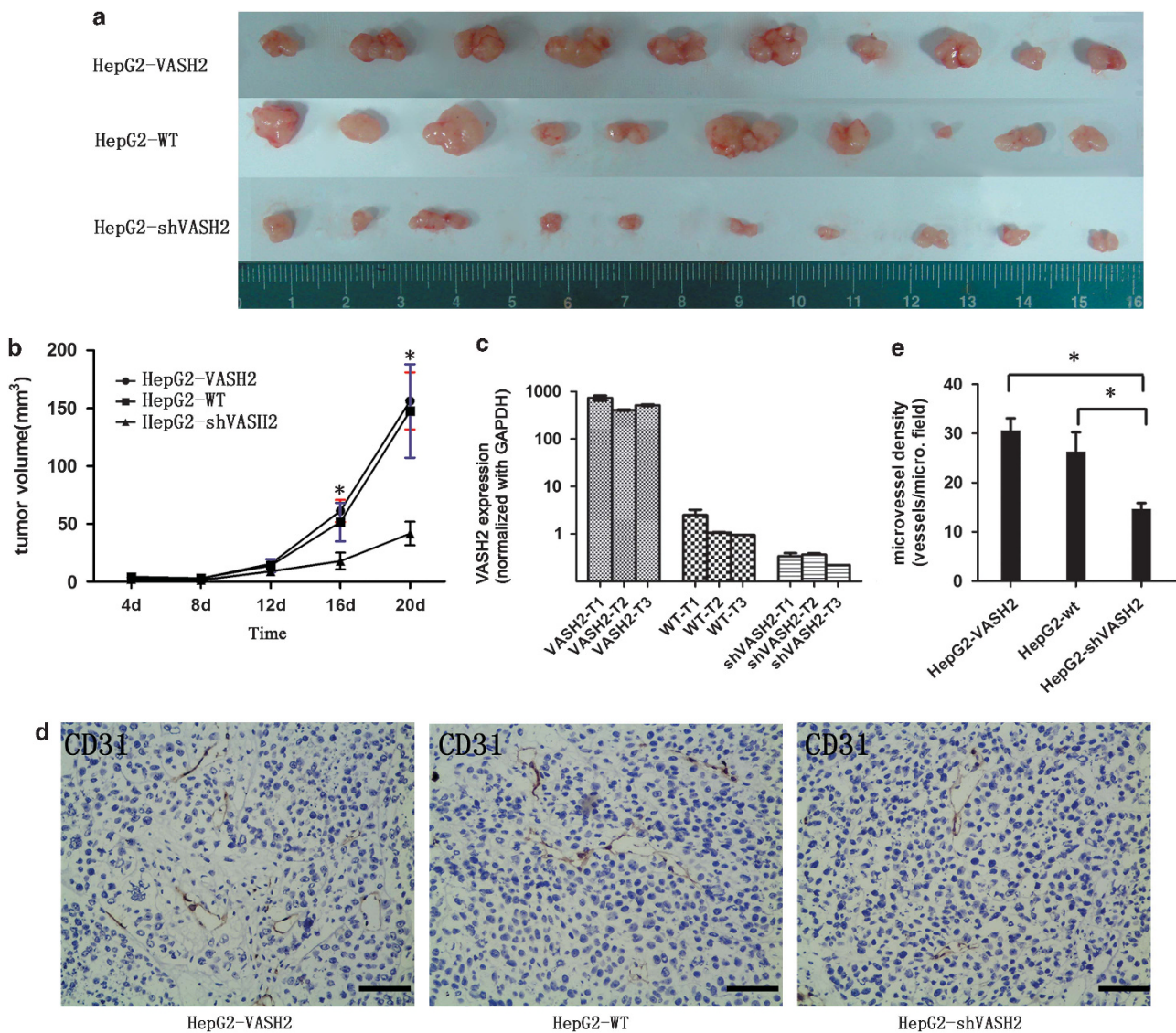


**Figure 7.** Subcutaneous injection of tumor cells. **(a)** HepG2-VASH2, HepG2-wt or HepG2-shVASH2 cells were suspended at a density of  $10^7$  cells/ml, and 100  $\mu$ l was bilaterally injected into the flank of nude mice ( $n = 5$ ). After 20 days the tumors were removed. The tumorigenesis rate was 100% for each group. The HepG2-shVASH2 tumors were smaller than those of the other groups, whereas the size of the HepG2-VASH2 tumors was not significantly different than that of the HepG2-WT tumors. **(b)** Tumor growth curves. After injection with tumor cells, the length and width of tumors were measured using vernier calipers every 4 days. The volume of the tumors was calculated using the equation  $\text{volume} = 1/2 \times \text{length} \times \text{width}^2$ . The data are presented as the average  $\pm$  s.d. of 10 tumors for each group. \*A significant difference between the groups when compared with the HepG2-shVASH2 group ( $P < 0.05$ ). **(c)** Three tumors from each group were resected, mRNA was extracted and VASH2 expression was measured using qRT-PCR. **(d)** CD31 immunohistochemistry was performed on the tumor tissue from the HepG2-VASH2, HepG2-WT and HepG2-shVASH2 groups. All scale bars represent 200  $\mu$ m; magnification,  $\times 20$ . **(e)** Microvessel density of CD31 immunohistochemistry. Each slide was evaluated with three fields, and data were analyzed as mean vessel number of these three fields.

that of VASH1: SVBP is prepared in advance and accumulates under or at the cell surface. Once VASH2 protein is available, it binds SVBP, which facilitates the secretion of VASH2. Interestingly, the expression of SVBP and that of VASH2 are independent of one another. Overexpression of VASH2 did not increase SVBP expression, which would, in turn, have helped to further enhance VASH2 secretion. This may partly explain why the overexpression groups in our study were similar to the HepG2-wt group. In addition, VASH2 secretion is increased  $\sim$ twofold following overexpression of SVBP. This suggests another mechanism, such as a cell surface channel or another chaperone, may assist VASH2 secretion. In addition, recombinant human VASH2 protein failed to promote tube formation of

HUVECs in our assay, which might be due to a lack of processing and secretion (data not shown).

We also found that, through autocrine and paracrine mechanisms, VASH2 enhanced the expression of FGF-2 and VEGF, which have direct angiogenic activity. This phenomenon may partly explain how VASH2 promotes angiogenesis. In addition, we found nuclear factor- $\kappa$ B was upregulated about  $1.7 \pm 0.25$ -fold in VASH2-overexpressing HCC cells. As nuclear factor- $\kappa$ B was reported to have a key role in angiogenesis by regulating transcription of angiogenic growth factors (such as VEGF and FGF),<sup>20,21</sup> we consider nuclear factor- $\kappa$ B signal may be the possible mechanisms of VASH2 to upregulate VEGF and FGF-2. At the same time, VASH1 is upregulated following VASH2 overexpression



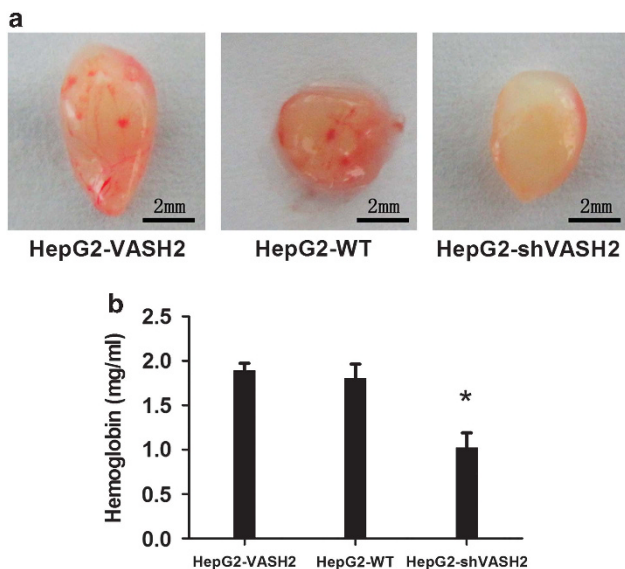


**Figure 8.** Matrigel plug assay. (a) Cells were suspended in Matrigel and DMEM and subcutaneously injected into the flanks of mice ( $n=3$ ). After 15 days, the Matrigel plugs were removed and photographed. Representative Matrigel plugs from the HepG2-VASH2, HepG2-wt and HepG2-shVASH2 groups are shown. (b) The relative amount of angiogenesis was analyzed based on the RBC hemoglobin level, determined using the Drabkin method. The relative hemoglobin content is the hemoglobin level (mg) divided by the final volume of each plug. The data are presented as the mean  $\pm$  s.d. for each group. \*A significant difference when compared with the HepG2-shVASH2 group ( $P<0.05$ ).

in HCC. This may be because angiogenic and anti-angiogenic factors are simultaneously activated during angiogenesis. However, the activity of the angiogenic factors is stronger than that of the anti-angiogenic factors. Our results are consistent with this hypothesis.

HCC, the most common primary liver tumor, relies on the formation of new blood vessels for growth. VEGF is critical for angiogenesis,<sup>22,23</sup> which has provided a strong rationale for anti-VEGF therapies.<sup>5</sup> However, the clinical use of VEGF inhibitors is more challenging than anticipated. Tumor angiogenesis can become VEGF-independent or even resistant to VEGF at more advanced stages because of the production of other angiogenic molecules.<sup>24,25</sup> In addition, anti-VEGF therapy has toxic vascular side effects such as proteinuria. In contrast with VEGF, VASH1, as a counter to VASH2, has been shown to both inhibit EC angiogenesis and protect EC from apoptosis. As a VEGF-independent and EC-extrinsic angiogenic factor, VASH2 is a novel target for anti-angiogenesis therapy.

In addition, VASH2 has been found to promote HCC cell proliferation in addition to angiogenesis. Therefore, VASH2 may exert other functions, such as invasion, which requires further study. Here, we mainly show the effects of VASH2 on HCC cells, we also have observed similar results in pancreatic cancer cells, indicating that VASH2 may function as an important tumor-associated gene in various solid tumors.

## MATERIALS AND METHODS

### HCC samples

Paired samples of cancerous liver tissue and adjacent non-cancerous liver tissue were obtained from 65 patients with HCC who underwent surgical resection at two centers (Jiangsu Province Hospital, China and Aichi Cancer Center Hospital, Nagoya, Japan) in accordance with the institutional policy. All patients provided written informed consent. In addition, samples of normal liver tissue were obtained from five patients who underwent a

partial hepatectomy for liver metastasis of primary colon cancer. Tissue samples were flash frozen and stored at  $-80^{\circ}\text{C}$ .

### Cell culture

Cells were maintained in DMEM (Gibco, 12100-046, Invitrogen, Carlsbad, CA, USA) containing 10% fetal bovine serum (Gibco, C2027-050, Uruguay), 100 mg/ml penicillin and 100 mg/ml streptomycin (Gibco, 15140122, Grand Island, NY, USA) at  $37^{\circ}\text{C}$  with 5%  $\text{CO}_2$ . Human liver cancer cells HepG2 and Hep3B were obtained from the American Type Culture Collection (Manassas, VA, USA). Huh7 and L02 cells were provided by Professor Beicheng Sun of the Department of General Surgery, The First Affiliated Hospital of Nanjing Medical University (Nanjing, China). HUVECs were purchased from KeyGEN in China (KG110, Nanjing, China).

### Plasmid construction and lentivirus packaging

VASH2 and SVBP lentiviral constructs were generated using PrimeSTAR HS DNA Polymerase (Takara, DR010A, Dalian, China) and the Lv-CMV-EGFP vector (the SVBP gene was fused with a V5 tag so that the V5 antibody could be used to measure VASH2 protein). shRNAs for human VASH2 were designed in our lab and constructed in pLKO.1-puro vectors. Three shRNA plasmids (sh1, sh2 and sh3) were constructed against different VASH2 targets, including a scrambled sequence as a negative control. All plasmids were verified by sequencing (Invitrogen). After infection with lentivirus, cells were tested for overexpression or knockdown of the VASH2 gene. For knockdown, one construct (sh2), with  $\geq 85\%$  knockdown efficiency, was used for further studies. The shRNA sequences used for further studies were as follows: shVASH2, 5'-CCGGTTTGACTTTGAGGACTCTTACCTCGAGGT AAGAGTCCTCAAAGTCAAATTTTG-3' and shScramble, 5'-CCGGCCTAAGGT TAAGTCGCCCTCGCTCGAGCGAGGGCGACTTAACCTTAGGTTTTTG-3'.

### Quantitative RT-PCR

Total RNA was extracted from cells and tissues using TRIzol reagent (Invitrogen, 15596-026), and cDNA was synthesized using Primescript RT Reagent (TAKARA). qRT-PCR was performed on a 7500 Real-Time-PCR System (Applied Biosystems, Carlsbad, CA, USA) using Taqman probes for GAPDH (Hs99999.m1, Applied Biosystems) and VASH2 (Hs00226928.m1). GAPDH was used as a reference to obtain the relative fold change for targets using the comparative Ct method.

### Growth, cell cycle and apoptosis analysis

Cell growth was measured using a modified 3-(4,5-dimethylthiazol-2-yl)-2,5-diphenyl tetrazolium bromide assay. Five groups of cells in logarithmic growth were seeded into 96-well plates. Each group was seeded in five duplicates. The cells were then cultured for 24, 48, 72, 96 or 120 h. Finally, the absorbance was measured using a microtiter plate reader (Tecan, Salzburg, Austria) with the 550 nm measuring wavelength and 620 nm reference wavelength. The growth of each group was calculated by averaging the optical density.

Cell cycle and apoptosis were performed as previously described by flow cytometry (Becton Dickinson, San Jose, CA, USA)<sup>26</sup>

### Tube formation

HepG2-VASH2-SVBP, HepG2-VASH2, HepG2-wt, HepG2-shVASH2 and HepG2-shcont cells were cultured as described above. When the cells reached 80% confluence, the culture medium was changed to DMEM without fetal bovine serum. After an additional 48 h culture, the supernatant was collected as CM and stored at  $-20^{\circ}\text{C}$ . After thawed at  $4^{\circ}\text{C}$  overnight, the Matrigel (BD, 356230, Bedford, MA, USA) was coated in 96-well plate then incubated at room temperature for at least 30 min to gel. HUVECs were suspended at a density of  $2 \times 10^5$  cells/ml in the different CMs. The cell suspensions (100  $\mu\text{l}$ ) were added to each Matrigel-coated well. DMEM was substituted for CM for the negative control. After 18 h, the formed networks were photographed and analyzed using Image-Pro Plus (Media Cybernetics, Bethesda, MD, USA) to calculate the area of network as described previously.<sup>27</sup>

### In vivo tumorigenesis experiments

Four-week-old male nude mice (BALB/cA-nu (nu/nu)) were purchased from the Shanghai Experimental Animal Center (Chinese Academy of Sciences, Shanghai, China). A total of 15 mice were randomly divided into three groups. HepG2-VASH2, HepG2-wt and HepG2-shVASH2 cells were

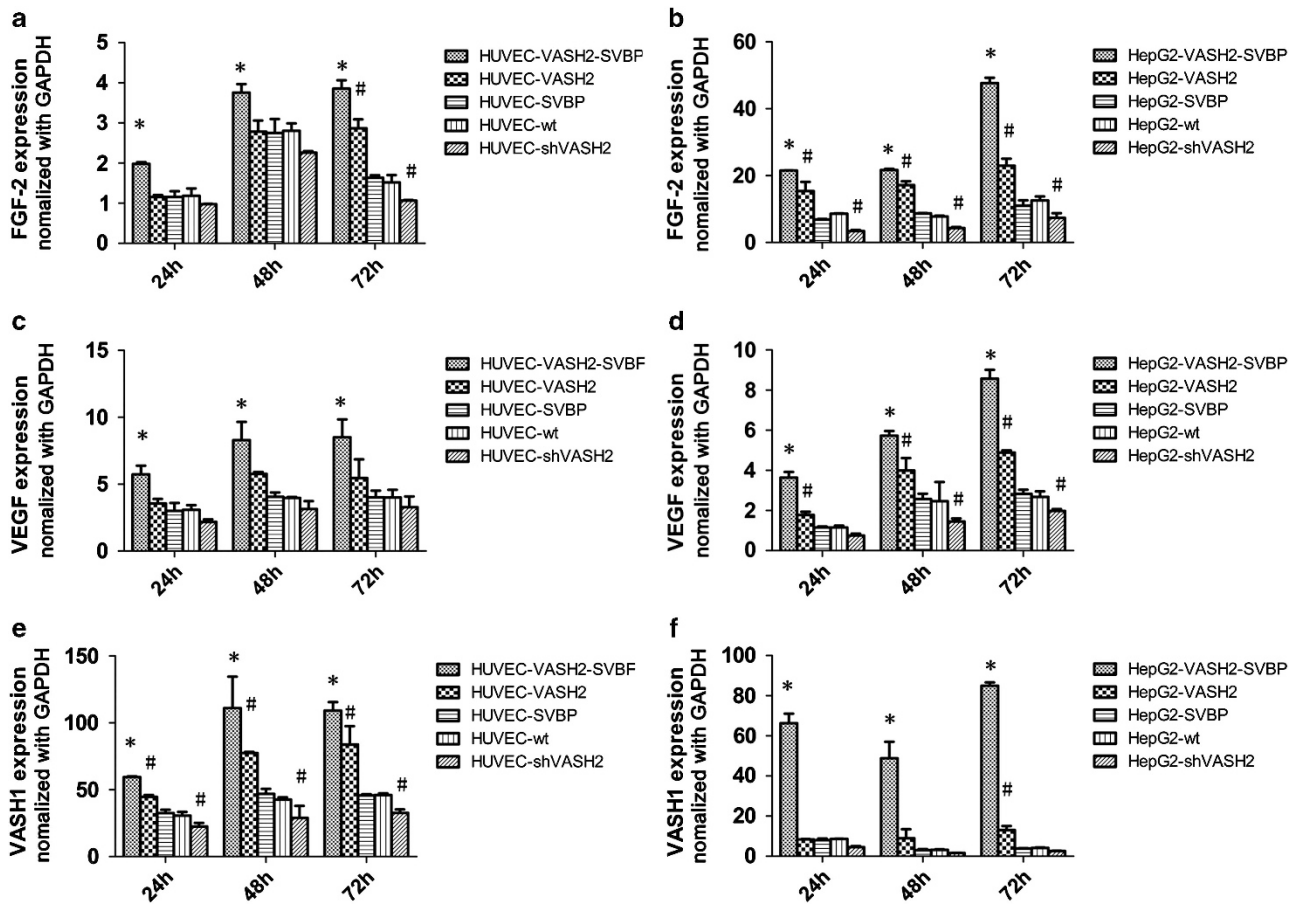


**Figure 9.** Expression of VASH2 with or without SVBP co-expression. VASH2 regulates the expression of FGF-2, VEGF and VASH1 in HUVECs and HepG2 cells in a coculture system. HepG2-VASH2-SVBP cells secreted the most VASH2 and increased the level of FGF-2 (a, b), VEGF (c, d) and VASH1 (e, f) both in HepG2 cells and HUVECs (\* $P < 0.05$  when compared with HepG2-VASH2). HepG2-shVASH2 CM decreased FGF-2 (a, b), VEGF (c, d) and VASH1 (e, f) expression at some time points (# $P < 0.05$  when compared with HepG2-wt).

bilaterally injected subcutaneously into the flanks of the mice ( $10^6$  cells/100  $\mu$ l per flank). Bidimensional tumor measurements were taken with calipers every 4 days, and the mice were euthanized after 20 days. The tumor volume was calculated using the formula (width<sup>2</sup>  $\times$  length)/2.

#### Matrigel plug angiogenesis assay

Nine male mice were randomly divided into three groups. HepG2-VASH2, HepG2-wt and HepG2-shVASH2 cells were resuspended at  $5 \times 10^7$  cells/ml in serum-free medium. Aliquots of cells (0.1 ml,  $5 \times 10^6$  cells) were mixed with 0.4 ml Matrigel and bilaterally injected into the flanks of each mouse (100  $\mu$ l cell mixture/per flank). Matrigel mixed with medium alone was used as a negative control. The Matrigel plugs were removed 15 days after implantation and used for the measurement of hemoglobin content using Drabkin's reagent (Sigma, D5941, St Louis, MO, USA). The data are presented as the mean  $\pm$  s.d. from replicate experiments.<sup>28</sup>

#### Immunohistochemistry and microvessel density analysis

Frozen tissue sections were fixed in acetone and methanol (1:1) for 10 min and were then rinsed. After blocking endogenous peroxides and proteins, slides were incubated with diluted rat-anti-mouse CD31 antibody (BD Pharmingen, 550274, Franklin Lakes, NJ, USA) for 2 h at 37  $^{\circ}$ C then incubated with horseradish peroxidase-conjugated goat-anti-rat secondary antibody (Santa Cruz, sc-2032, Santa Cruz, CA, USA) for 1 h at 37  $^{\circ}$ C, incubated with a 3,3'-diaminobenzidine solution for 10 min and counterstained with hematoxylin.

Staining against the endothelial marker CD31 by means of immunohistochemistry was followed by observation under low magnification scope ( $\times 10$ ). Tumor slides were examined in a blinded manner and representative areas of vital tumor were selected for examination. Each

slide was evaluated with three fields, and data were analyzed as mean vessel number of these three fields.<sup>29</sup>

#### Western blot

Cell lysates were prepared by extracting protein with radioimmuno precipitation assay buffer. Membranes were blocked in 5% non-fat dried milk and incubated overnight at 4  $^{\circ}$ C with appropriate primary antibodies (the mouse-anti-human VASH2 monoclonal antibody utilized in western blot was described previously<sup>11</sup>). GAPDH (AG019-1, Beyotime, Nantong, China).

#### Dual luciferase reporter assay

Overlapping segments surrounding the TSS of the VASH2 gene were amplified and ligated into the pGL3 basic vector. The plasmids were co-transfected with the Renilla luciferase expression plasmid into HepG2 cells. After 48 h, cells were collected and luciferase activity was measured using the Dual Luciferase Reporter Assay System (Promega, E1910, Madison, WI, USA). The relative promoter activity was calculated as firefly fluorescence/Renilla fluorescence.

#### Chromatin immunoprecipitation

We carried out a ChIP assay according to instructions from Upstate Biotechnology. The following antibodies were used as follows: anti-trimethyl-histone H3 (lys4) antibody (07-473, Upstate Biotechnology, Lake Placid, NY, USA), anti-trimethyl-histone H3 (lys27) antibody (17-622, Upstate) and anti-acetyl-histoneH3 antibody (17-615, Upstate). Normal rabbit immunoglobulin G was used as a 'no antibody' control. Real-time-PCR was performed with SYBR Premix EX Taq (Takara). The amount of immunoprecipitated DNA was normalized to the input DNA as the following formula:  $\Delta Ct_{(normalized\ ChIP)} = (Ct_{(ChIP)} - Ct_{(input)}) - \log_2(\text{input dilution factor})$ , %Input =  $2^{(-\Delta Ct_{(normalized\ ChIP)})}$ . Average relative amount of

each amplified product was calculated from two independent ChIP experiments and a total of four independent PCR analyses.

### Enzyme-linked immunosorbent assay

To quantify the secretion of VASH2, an enzyme-linked immunosorbent assay kit (Huili Biotech, DZE11701, Changchun, China) was used to measure secreted VASH2. The samples analyzed were cell supernatants from HepG2-VASH2-SVBP and HepG2-VASH2 cells collected after 24, 48 or 72 h of culture. The cell numbers in each dish were counted to normalize the levels measured in the two groups. First, a standard was diluted to different concentrations to generate a standard curve. The supernatants were diluted sixfold with sample diluent and added to wells. After incubating at 37 °C for 30 min and washing five times, 50 µl horseradish peroxidase-conjugate reagents was added to each well except the blank. The plate was then incubated at 37 °C and washed as above. Chromogen Solution A and Chromogen Solution B (Huili Biotech, Changchun, China) were added to each well and incubated for 15 min in the dark. Finally, 50-µl stop solution was added to each well to stop the reaction. The optical density was read at 450 nm. The data are reported as concentration × 6/cell number (ng/ml/10<sup>6</sup> cells).

### Coculture assay

HUVECs and HepG2 cells expressing different levels of VASH2 were cocultured using six-well modified Boyden chambers with 0.4 µm pores (Corning, 3412, New York, NY, USA). HepG2 cells were plated in the lower chambers and HUVECs were seeded in the upper chambers. After the cells adhered, the culture medium was changed to serum-free DMEM, and the upper chambers containing the HUVECs were transferred to the plates with HepG2 cells. After coculture for 24, 48 or 72 h, RNA was isolated from both the HepG2 cells and the HUVECs. The expression of the angiogenesis factors FGF-2, VEGF and VASH1 was analyzed. Primers are available on request.

### Statistical analysis

All experiments were repeated in triplicate in this article. Where indicated statistical significance was determined by the Student's *t*-test. *P*-values <0.05 were considered as statistically significant.

### CONFLICT OF INTEREST

The authors declare no conflict of interest.

### ACKNOWLEDGEMENTS

We are very grateful to Professor Yujie Sun from Nanjing Medical University for continuous technical support. This work was supported by grants from the National Nature Science Foundation of China (no. 81172267 and 30901627).

### REFERENCES

- 1 Semela D, Dufour JF. Angiogenesis and hepatocellular carcinoma. *J Hepatol* 2004; **41**: 864–880.
- 2 Eggert A, Ikegaki N, Kwiatkowski J, Zhao H, Brodeur GM, Himmelstein BP. High-level expression of angiogenic factors is associated with advanced tumor stage in human neuroblastomas. *Clin Cancer Res* 2000; **6**: 1900–1908.
- 3 Doger FK, Meteoglu I, Tuncyurek P, Okyay P, Cevikel H. Does the EGFR and VEGF expression predict the prognosis in colon cancer? *Eur Surg Res* 2006; **38**: 540–544.
- 4 Cha HJ, Lee HH, Chae SW, Cho WJ, Kim YM, Choi HJ et al. Tristetraprolin down-regulates the expression of both VEGF and COX-2 in human colon cancer. *Hepatogastroenterology* 2011; **58**: 790–795.
- 5 Folkman J. Angiogenesis: an organizing principle for drug discovery? *Nat Rev Drug Discov* 2007; **6**: 273–286.
- 6 Llovet JM, Ricci S, Mazzaferro V, Hilgard P, Gane E, Blanc JF et al. Sorafenib in advanced hepatocellular carcinoma. *N Engl J Med* 2008; **359**: 378–390.
- 7 Zhu AX, Duda DG, Sahani DV, Jain RK. HCC and angiogenesis: possible targets and future directions. *Nat Rev Clin Oncol* 2011; **8**: 292–301.
- 8 Watanabe K, Hasegawa Y, Yamashita H, Shimizu K, Ding Y, Abe M et al. Vasohibin as an endothelium-derived negative feedback regulator of angiogenesis. *J Clin Invest* 2004; **114**: 898–907.
- 9 Yoshinaga K, Ito K, Moriya T, Nagase S, Takano T, Niikura H et al. Roles of intrinsic angiogenesis inhibitor, vasohibin, in cervical carcinomas. *Cancer Sci* 2011; **102**: 446–451.
- 10 Tamaki K, Moriya T, Sato Y, Ishida T, Maruo Y, Yoshinaga K et al. Vasohibin-1 in human breast carcinoma: a potential negative feedback regulator of angiogenesis. *Cancer Sci* 2009; **100**: 88–94.
- 11 Shibuya T, Watanabe K, Yamashita H, Shimizu K, Miyashita H, Abe M et al. Isolation and characterization of vasohibin-2 as a homologue of VEGF-inducible endothelium-derived angiogenesis inhibitor vasohibin. *Arterioscler Thromb Vasc Biol* 2006; **26**: 1051–1057.
- 12 Kimura H, Miyashita H, Suzuki Y, Kobayashi M, Watanabe K, Sonoda H et al. Distinctive localization and opposed roles of vasohibin-1 and vasohibin-2 in the regulation of angiogenesis. *Blood* 2009; **113**: 4810–4818.
- 13 Strahl BD, Allis CD. The language of covalent histone modifications. *Nature* 2000; **403**: 41–45.
- 14 Jenuwein T, Allis CD. Translating the histone code. *Science* 2001; **293**: 1074–1080.
- 15 Santos-Rosa H, Schneider R, Bannister AJ, Sherriff J, Bernstein BE, Emre NC et al. Active genes are tri-methylated at K4 of histone H3. *Nature* 2002; **419**: 407–411.
- 16 Plath K, Fang J, Mlynarczyk-Evans SK, Cao R, Worringer KA, Wang H et al. Role of histone H3 lysine 27 methylation in X inactivation. *Science* 2003; **300**: 131–135.
- 17 Gorisch SM, Wachsmuth M, Toth KF, Lichter P, Rippe K. Histone acetylation increases chromatin accessibility. *J Cell Sci* 2005; **118**(Part 24): 5825–5834.
- 18 Suzuki Y, Kobayashi M, Miyashita H, Ohta H, Sonoda H, Sato Y. Isolation of a small vasohibin-binding protein (SVBP) and its role in vasohibin secretion. *J Cell Sci* 2010; **123**(Part 18): 3094–3101.
- 19 Palacios D, Mozzetta C, Consalvi S, Caretti G, Saccone V, Proserpio V et al. TNF/p38alpha/polycomb signaling to Pax7 locus in satellite cells links inflammation to the epigenetic control of muscle regeneration. *Cell Stem Cell* 2010; **7**: 455–469.
- 20 Tammali R, Reddy AB, Srivastava SK, Ramana KV. Inhibition of aldose reductase prevents angiogenesis *in vitro* and *in vivo*. *Angiogenesis* 2011; **14**: 209–221.
- 21 Mi J, Zhang X, Liu Y, Reddy SK, Rabbani ZN, Sullenger BA et al. NF-kappaB inhibition by an adenovirus expressed aptamer sensitizes TNFalpha-induced apoptosis. *Biochem Biophys Res Commun* 2007; **359**: 475–480.
- 22 Yang ZF, Poon RT. Vascular changes in hepatocellular carcinoma. *Anat Rec (Hoboken)* 2008; **291**: 721–734.
- 23 Wu XZ, Xie GR, Chen D. Hypoxia and hepatocellular carcinoma: the therapeutic target for hepatocellular carcinoma. *J Gastroenterol Hepatol* 2007; **22**: 1178–1182.
- 24 Jain RK, Duda DG, Clark JW, Loeffler JS. Lessons from phase III clinical trials on anti-VEGF therapy for cancer. *Nat Clin Pract Oncol* 2006; **3**: 24–40.
- 25 Sitohy B, Nagy JA, Jaminet SC, Dvorak HF. Tumor surrogate blood vessel subtypes exhibit differential susceptibility to anti-VEGF therapy. *Cancer Res* 2011; **71**: 7021–7028.
- 26 Wang F, Xue X, Wei J, An Y, Yao J, Cai H et al. hsa-miR-520h downregulates ABCG2 in pancreatic cancer cells to inhibit migration, invasion, and side populations. *Br J Cancer* 2010; **103**: 567–574.
- 27 Eccles SA, Court W, Patterson L, Sanderson S. *In vitro* assays for endothelial cell functions related to angiogenesis: proliferation, motility, tubular differentiation, and proteolysis. *Method Mol Biol* 2009; **467**: 159–181.
- 28 Liu LZ, Fang J, Zhou Q, Hu X, Shi X, Jiang BH. Apigenin inhibits expression of vascular endothelial growth factor and angiogenesis in human lung cancer cells: implication of chemoprevention of lung cancer. *Mol Pharmacol* 2005; **68**: 635–643.
- 29 Weidner N. Current pathologic methods for measuring intratumoral microvessel density within breast carcinoma and other solid tumors. *Breast Cancer Res Treat* 1995; **36**: 169–180.

Supplementary Information accompanies the paper on the Oncogene website (<http://www.nature.com/onc>)